NDT&E International 121 (2021) 102440

Contents lists available at ScienceDirect

NDT and E International

journal homepage: http://www.elsevier.com/locate/ndteint

Orthogonally polarised shear waves for evaluating anisotropy and cracks in metals

Jaime Parra-Raad, Bo Lan, Frederic Cegla *

NDE Group, Mechanical Engineering Department, Imperial College London, Exhibition Road, South Kensington, SW7 2AZ, United Kingdom

ARTICLE INFO

Keywords:
Anisotropic material
Polarised shear waves
Crack detection
Orthogonal co-located coils (OCLC)
EMATs
Principal shear directions
Material characterisation
Crack characterisation

ABSTRACT

The detection of crack-like defects using ultrasound is a problem widely studied by the non-destructive evaluation community. In this work, a technique of how to detect the presence of a crack-like defect and estimate its orientation in an anisotropic material by means of two orthogonal shear waves is presented. A detailed study of shear wave propagating and splitting at any incident angle, and its interaction with crack-like defects in anisotropic materials, is also presented. In this paper it is shown that by the use of two orthogonal shear waves with linear polarisation the authors could: 1) estimate the material level of anisotropy within approximately 0.5% of the measured value; 2) estimate the angular position of the principal shear directions of the material with respect to the orthogonal shear wave sources within $\pm 5^{\circ}$ accuracy; 3) excite a shear wave purely polarised along one of the principal shear directions with two orthogonal shear waves placed at an arbitrary angular position; 4) detect the presence of a crack-like defect in an anisotropic material based on the back-wall echoes of two orthogonal shear waves, 5) estimate the orientation of a crack-like defect in an anisotropic material within $\sim \pm 5^{\circ}$ of the theoretical value. The simulation and experimental results obtained show that the technique presented in this paper has potential to become an effective tool for crack-like defect detection and material characterisation.

1. Introduction

Shear waves are important in Non-Destructive Evaluation (NDE) for assessing material microstructure [1–3], detecting and sizing crack defects [4–8], or even measuring residual stresses [9–11], due to their higher sensitivity to these features compared to longitudinal waves. The elastic anisotropy (i.e. direction-dependence) of materials, which is a general phenomenon in metals and minerals alike, strongly affects the propagation of shear waves [12] by causing the so-called wave splitting: a shear wave with an arbitrary polarisation/shear direction would split into two partial shear waves with polarisation along the two principal shear directions (PSDs) of the material, and the partial waves then travel into the material at different wave speeds [13].

Shear splitting greatly complicates the inspections in anisotropic materials, since both time-domain signals and amplitude drops now need to be carefully handled for defect detection and sizing [14–18]. Whereas in an isotropic material these factors only depend on the source position and the defect, in an anisotropic material there is also a dependence on the relative orientation with respect to the PSDs. These PSDs can be arbitrarily oriented with respect to surfaces of the component that is being tested, which further complicates the detection procedure.

In a previous study, the authors presented a method for simultaneous crack detection and thickness measurement in a metallic material [16]. The proposed methodology utilised two orthogonal shear waves with linear polarisation to inspect the material. The thickness of the material was estimated by calculating the product of Time-of-Flight (ToF) of the back-wall echoes and the shear wave speed in the material. The presence of a crack-like defect was determined by comparing the amplitude of the first back-wall echoes of the two orthogonal shear waves. The study focused on the interaction of the two shear waves of different polarisation with a crack-like defect in an aluminium block. The previous work relied on two assumptions: 1) the material that is being inspected is isotropic 2) any signal amplitude difference is the result of the presence of a defect. However, both assumptions are usually violated. Even aluminium, which is normally considered an isotropic material, exhibits weakly anisotropic behaviour [19]; and in anisotropic materials, the wave splitting phenomenon introduces signal amplitude drops similar to

* Corresponding author.
E-mail address: f.cegla@imperial.ac.uk (F. Cegla).

https://doi.org/10.1016/j.ndteint.2021.102440
Received 24 July 2020; Received in revised form 28 September 2020; Accepted 19 March 2021
Available online 2 April 2021
0963-8695/© 2021 The Author(s). Published by Elsevier Ltd. This is an open access article under the CC BY-NC-ND license (http://creativecommons.org/licenses/by-nc-nd/4.0/).

those obtained when a defect is present.

The wave propagation physics to address these considerations are presented in this paper. The study will explain how two orthogonal and linearly polarised shear waves propagate in anisotropic materials and how their signal amplitude is affected by the presence of a crack-like defect. We will demonstrate a convenient and accurate way to identify the PSDs of an anisotropic material, using an electro-magnetic acoustic transducer (EMAT) with a pair of co-located and orthogonally aligned coils known as the orthogonal co-located coils EMAT or OCLC-EMAT. With the four time-domain signals obtained from the transducer, a shear wave with pure polarisation (along one of the PSD) can be generated, and indeed the shear waves excited with any arbitrary polarisation can be reconstructed (we call it electrical steering). It will then be shown that, with the PSDs known, we can not only detect the presence of a crack-like defect in an anisotropic material, but also accurately and reliably evaluate the orientation of the crack.

2. Background and context

The experiments in this paper were executed with the same setup as described in Ref. [16]. In this setup, the OCLC-EMAT is used to excite two orthogonal and linearly polarised shear waves, at the same location in space. The transducer is composed of a magnetic circuit and two butterfly coils, one on top of the other, at the same location. However, one of the coils is rotated by 90° with respect to the other.

The main advantage of the OCLC-EMAT is the orientation of its butterfly coils. Their orientations permit the induction of two orthogonal and independent eddy currents in the surface of a conductive material. In combination with the bias magnetic field, the OCLC-EMAT can simultaneously excite two linearly polarised surface loads in orthogonal directions at the same spatial location via the Lorentz force [20].

The previous work [16] assumed that the inspected aluminium block was an isotropic material. However, the ToFs of the two orthogonal shear waves showed that the waves travelled at different wave speeds. The difference of wave velocity was reported to be $27m/s$ for the aluminium block that was used. The OCLC-EMAT was used to excite two shear waves with orthogonal orientation on top of the aluminium block, as shown in Fig. 1a and Fig. 1b.

The difference of wave speed is hardly noticeable on the first back-wall echo. However, when the time-traces of several back-wall echoes are plotted, the difference in speed becomes noticeable. To illustrate this, Fig. 2a shows two newly acquired time-traces of 12 back-wall echoes obtained at the same location, including a close up view of the 1^{st} and 7^{th} pair of back-wall echoes excited with the OCLC-EMAT. These two close up views show the difference in arrival time of the back-wall echoes increasing as the time passes.

In the previously reported work, the authors used the relative signal amplitude of the two back-wall echoes to deduce the presence of a crack and to estimate its size. The existence of a signal amplitude difference among the two back-wall echoes was assumed to be induced only by the presence of the defect. However, the amplitude of the back-wall echoes when two orthogonal shear waves interact with a crack-like defect depends on the morphology of the defect and the relative angle between the polarisation direction of the excitation sources and the PSDs of the material [21]. When the relative angle between the PSDs and the transducers is 0°, the interaction of the two orthogonal shear waves with a crack-like defect behaves as if the material was isotropic and, therefore the method proposed previously [16] can be used to detect and estimate the defect. However, when the angle is different to 0°, the back-wall signal amplitude depends not only on the morphology of the crack but also on the orientation of the transducer with respect to the PSDs. The effect of the angle between the excitation polarisation and the PSDs can be seen by comparing the time-traces obtained when the polarisation direction of excitation is changed with respect to the PSDs. Fig. 2a and b illustrate the effect of having a source oriented at an angle of 0° and 60°,

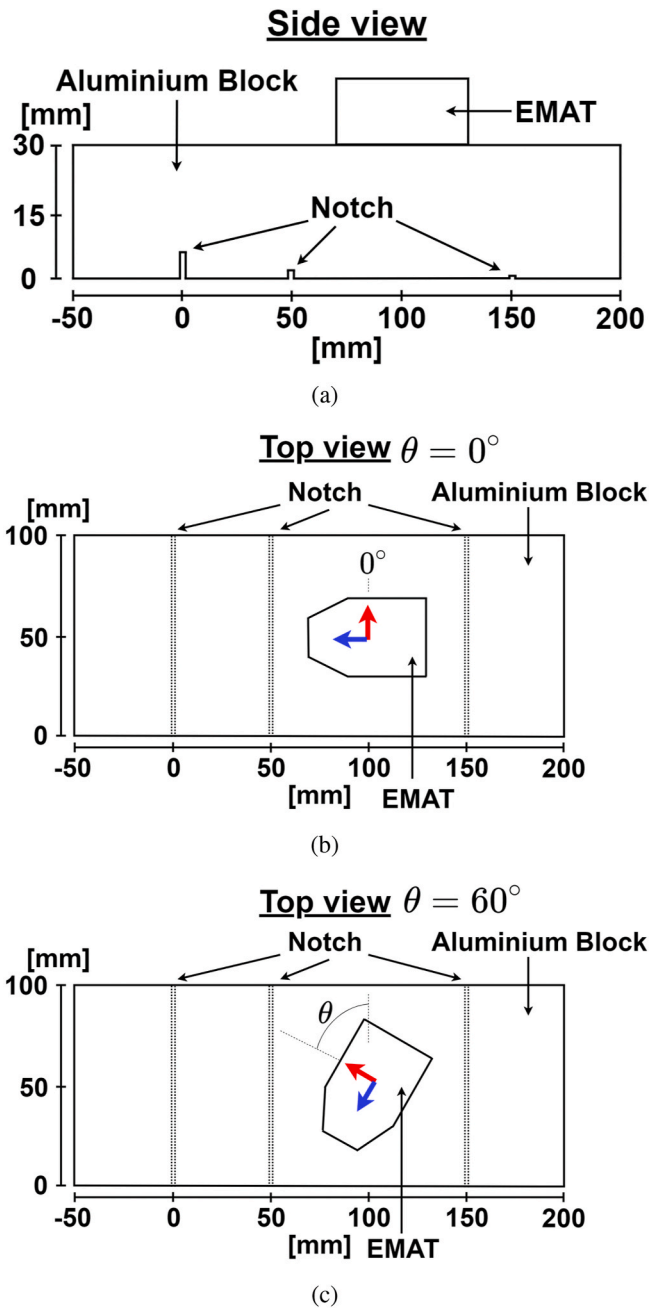
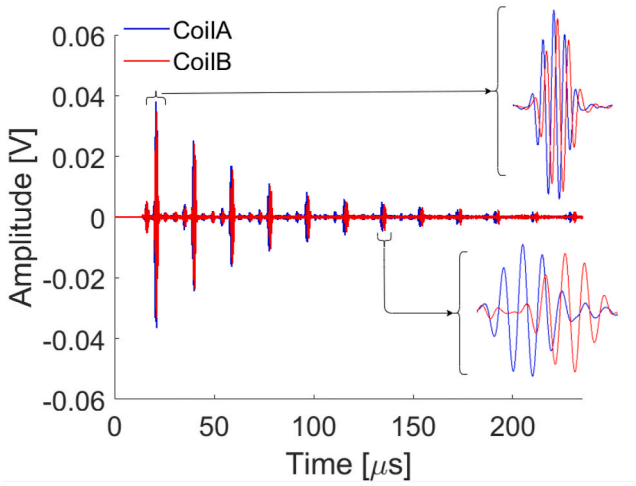
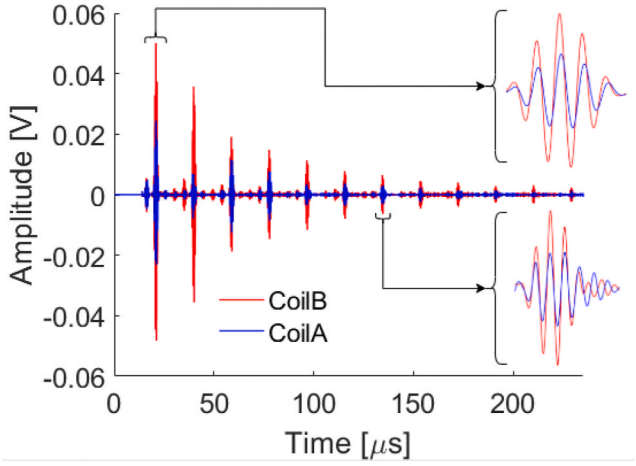


Fig. 1. Schematic of the orthogonal co-located coils EMAT positioning on the aluminium block. a) Side view schematic of the OCLC EMAT on top of the aluminium block. b) Top view schematic of the OCLC EMAT on top of the aluminium block. c) Top view schematic of the OCLC EMAT 60° rotated on top of the aluminium block. The θ indicates the rotated angle of the EMAT's coils with respect of the principal shear directions. The blue and red arrows indicate the shear polarisation of coil A and coil B, respectively. The 60° indicates the alignment with the principal shear directions of the material. (For interpretation of the references to colour in this figure legend, the reader is referred to the Web version of this article.)

respectively (the second source orientation was selected arbitrarily). Fig. 1c displays a schematic of the OCLC-EMAT coils rotated by 60° with respect to the PSDs and Fig. 2b shows the time-traces obtained when the OCLC-EMAT is rotated by 60°. The amplitudes of the echoes have considerably changed, especially those of coil A. The experimental results shown in Fig. 2b were obtained at the same location as those in Fig. 2a, only the transducer orientation was changed. During both tests the shear waves were excited simultaneously.



(a)



(b)

Fig. 2. Back-wall reflections measured with the coils at different OCLC-EMAT orientation. The A-scans were obtained by placing the OCLC-EMAT coils at $\theta = 0^{\circ}$ and $\theta = 60^{\circ}$ with respect to the principal shear directions. a) A-scans excited and measured with the OCLC-EMAT coil at $\theta = 0^{\circ}$. b) A-scans excited and measured with the OCLC-EMAT coils at $\theta = 60^{\circ}$.

These observations highlight that the transducer orientation relative to the PSDs influences the back-wall echo amplitudes as much as the presence of a crack. While the orientation of the PSDs can be determined by carefully rotating a transducer on the surface to find the maximum reflection amplitude, it is tedious to do this by hand consistently. In the next sections, we will explore how the orientation of the probe relative to the PSDs can be determined without needing to physically rotate the transducer, how to use this information to electrically steer a shear wave, how to detect the presence of a crack and how to characterise the crack orientation in the material.

3. Transmission and measurement of orthogonal shear waves in anisotropic materials

When a shear wave starts propagating in an anisotropic material, the strain of the wave splits into two different strain components [12]. These strain components travel with polarisation along the principal shear directions of the material and are orthogonal and independent of each other. Their displacement produces two different shear waves travelling along the direction of propagation of the initial shear wave, as shown in Fig. 3. Fig. 3 illustrates the wave splitting phenomenon of an excited

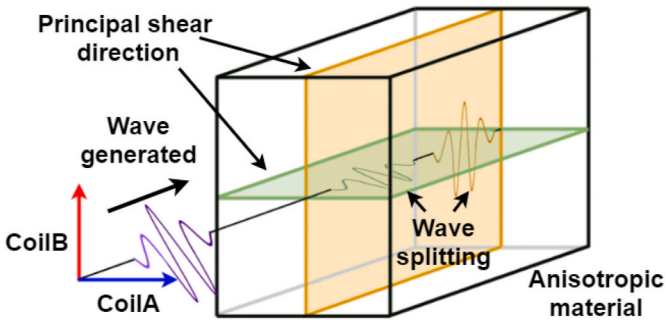


Fig. 3. Wave splitting into two shear waves when travelling through an anisotropic medium. The new shear waves will travel aligned with the principal shear directions. The blue and red arrows indicate the direction of forcing that coil A and B, respectively, will induce on the specimen. (For interpretation of the references to colour in this figure legend, the reader is referred to the Web version of this article.)

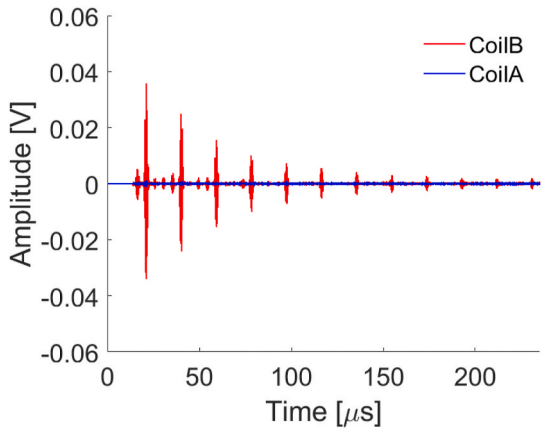
shear wave with arbitrary polarisation propagating in an anisotropic material. The shear wave was assumed to be excited with the OCLC-EMAT.

The split waves can have different amplitude and wave speed, depending on the properties of the material [22] and the polarisation direction of the incident shear wave. The material characteristics affect the wave speed at which the two waves travel in the material. The polarisation direction determines how the energy of the incident wave splits across the two PSDs. To illustrate the effect of the polarisation angle on a shear wave propagating in an anisotropic material, two different pulse-echo tests were performed on the same area of an aluminium block. The location used was the same as the one used for the results of Fig. 2. The first pulse-echo test was carried out by using the OCLC-EMAT coil B to generate a shear load at the surface of the aluminium block. The surface load was polarised along the principal shear direction 1 ($\theta = 0^{\circ}$, orientation shown in Fig. 1b). The second pulse-echo test was performed by exciting one surface load with the OCLC-EMAT coil B at an angle of 60° from principal shear direction 1 ($\theta = 60^{\circ}$, orientation shown in Fig. 1c). The back-wall echoes of the two pulse-echo tests were recorded using both coils of the OCLC-EMAT. The results of the two pulse-echo tests are displayed in Fig. 4.

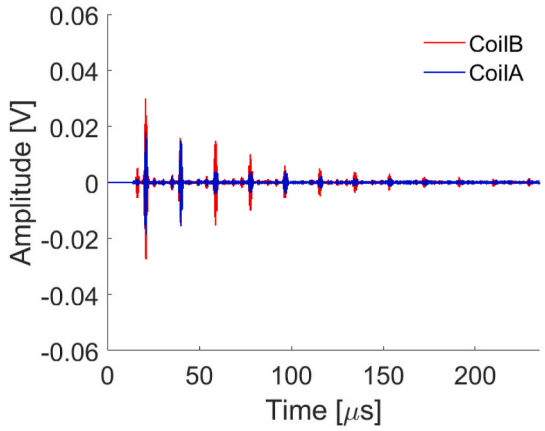
In Fig. 4a, it can be observed that the back-wall echoes of the incident shear wave were recorded by coil B, only. The reason for this is that the excited wave was polarised along the principal shear direction 1 of the material. Therefore, its back-wall echoes were measured with the coil aligned with this PSD. While in Fig. 4b it is observed that the back-wall echoes of the generated shear wave were recorded with the two coils of the OCLC-EMAT. This phenomenon can be explained by wave splitting in an anisotropic material. The strain of the shear wave that coil B generated was polarised 60° with respect to PSD 1, so when the wave started to propagate in the material, the strain of the incident wave split into two strain components; which are polarised along the principal shear directions. When these two waves bounced back from the back-wall to the OCLC-EMAT their strain components generate particle displacement in the material that can be measured by both coils of the EMAT.

3.1. Physics of shear waves propagation in anisotropic media

To understand how two orthogonal shear waves travel through an anisotropic material, the phenomenon of the waves propagating in the material is treated as strain vectors projecting onto two orthogonal systems of coordinates. The two orthogonal systems of coordinates indicate the PSDs of the material and the excitation source and/or wave receivers. A shear wave can have one or two strain components depending on its orientation with respect to the anisotropic material. The projection of the strain vectors of the orthogonal shear sources onto



(a)



(b)

Fig. 4. Back-wall reflections obtained by exciting solely Coil B of the OCLC-EMAT. a) A-scans measured when the OCLC-EMAT is align with the principal shear directions. b) A-scans measured when the OCLC-EMAT coils are 60° rotated with respect to the principal shear directions.

the PSDs dictated how the strain of each source splits into the material. Then the projection of the strain onto the axes of the measurement system represents how the two orthogonal shear waves are recorded by the receivers. Therefore, the polarisation directions and amplitudes of the split partial waves obey the rules of vector addition/projection, and can be treated by relatively simple vector operations, where the signal detected by the coils are the projections of the partial waves along the coil orientations.

Fig. 5 shows the phenomenon of one shear wave with linear polarisation generated by coil B of the OCLC-EMAT propagating into an anisotropic material. The propagation of the shear wave and its back-wall echoes are represented as vector quantities projected onto two orthogonal systems, one represents the PSDs and the other the OCLC-EMAT coils. The strain vectors represent the shear wave strain at its maximum amplitude. Additionally, the labels Coil B and Coil A orientation indicate the orientation of the force generated by the coils. θ indicates the angle between the two orthogonal systems. Fig. 5a presents the strain generated by coil B on top of the anisotropic material as a vector quantity. The strain vector is aligned with the force orientation generated by coil B. Fig. 5b shows how the strain generated by coil B is split onto the PSDs. These strains then travel as two independent shear waves polarised along the PSDs into the material. Fig. 5c illustrates the projections of the strain components of the returning shear waves onto the orientation of the coils of the OCLC-EMAT at the surface of the material. Fig. 5d shows the vector quantities of the strain components that are measured by the coils of the OCLC-EMAT at the first back-wall echo of the excited shear wave in Fig. 5a. V indicates the wave speed of each strain vector. The sub-indices 1 and 2 are used to indicate the velocity of waves that travel with polarisations corresponding to each of the PSDs.

Based on the strain vector representation of a shear wave propagating through the anisotropic material shown in Fig. 5, the maximum amplitude of the back-wall echoes measured by the OCLC-EMAT coils can be described as:

$$S_{coilB\rightarrow coilB} = A^*\left[cos^2(\theta) + sin^2(\theta) * e^{(i\omega\delta t)}\right] \tag{1}$$

$$S_{coilB\rightarrow coilA} = A^*[sin(\theta)^*cos(\theta) + sin(\theta)^*cos(\theta)^*e^{(i\omega\delta t)}] \tag{2}$$

$$S_{coilA\rightarrow coilB} = A^*[sin(\theta)^*cos(\theta) + sin(\theta)^*cos(\theta)^*e^{(i\omega\delta t)}] \tag{3}$$

$$S_{coilA\rightarrow coilA} = A^*\left[sin^2(\theta) + cos^2(\theta) * e^{(i\omega\delta t)}\right] \tag{4}$$

Where variables $S_{coilB\rightarrow coilB}$ and $S_{coilB\rightarrow coilA}$ represent the signal amplitude of the back-wall echoes received by the OCLC-EMAT coils when coil B is used to excite a shear load in an anisotropic material and its back-wall echoes are measured by coil B and coil A, respectively. $S_{coilA\rightarrow coilB}$ and $S_{coilA\rightarrow coilA}$ are the back-wall signals measured by coil B and coil A when coil A is used to generate a shear load in an anisotropic material. A indicates the maximum amplitude of the strain components that the OCLC-EMAT coils excite on the surface of the anisotropic material. For coil A and coil B, the strain components generated on top of the material are assumed to be equal in magnitude. The difference in wave speed among the two shear waves propagating along the PSDs is accounted for by $e^{(i\omega\delta t)}$; where ω is the angular frequency of the shear waves, δt is the time difference between arrivals of waves travelling along the two different PSDs and i is $\sqrt{-1}$.

3.2. Detection of the principal shear directions using two orthogonal and co-located shear transducers

The splitting of shear loads into two orthogonal shear waves can be used to determine the orientation of the principal shear components in an anisotropic material. The angle between the two orthogonal systems, defined as θ, can be estimated from equations (1)–(4). First subtract equation (4) from equation (1):

$$C = S_{coilB\rightarrow coilB} - S_{coilA\rightarrow coilA}$$
$$C = A^*\left[cos(2\theta) - cos(2\theta)^*e^{(i\omega\delta t)}\right] \tag{5}$$

then sum equation (2) and equation (3):

$$D = S_{coilB\rightarrow coilA} + S_{coilA\rightarrow coilB}$$
$$D = A^*\left[sin(2\theta) + sin(2\theta)^*e^{(i\omega\delta t)}\right] \tag{6}$$

The angle can be estimated as:

$$tan(2\theta) = D/C = max(D)/max(C)$$
$$\theta = \frac{tan^{-1}(max(D)/max(C))}{2} \tag{7}$$

Where *max* indicates the maximum absolute value of the first back-wall echo of the measured signals.

3.3. Exciting a shear wave polarised along one PSD and general electrical steering

For conventional measurements, one normally needs to rotate the transducer to find the PSDs, and then align the transducer with the PSDs to excite a shear wave polarised along one of the PSDs. We have shown that with the OCLC-EMAT we can find the PSDs simply from one set of signals, and now we will demonstrate that this same set of signals can be

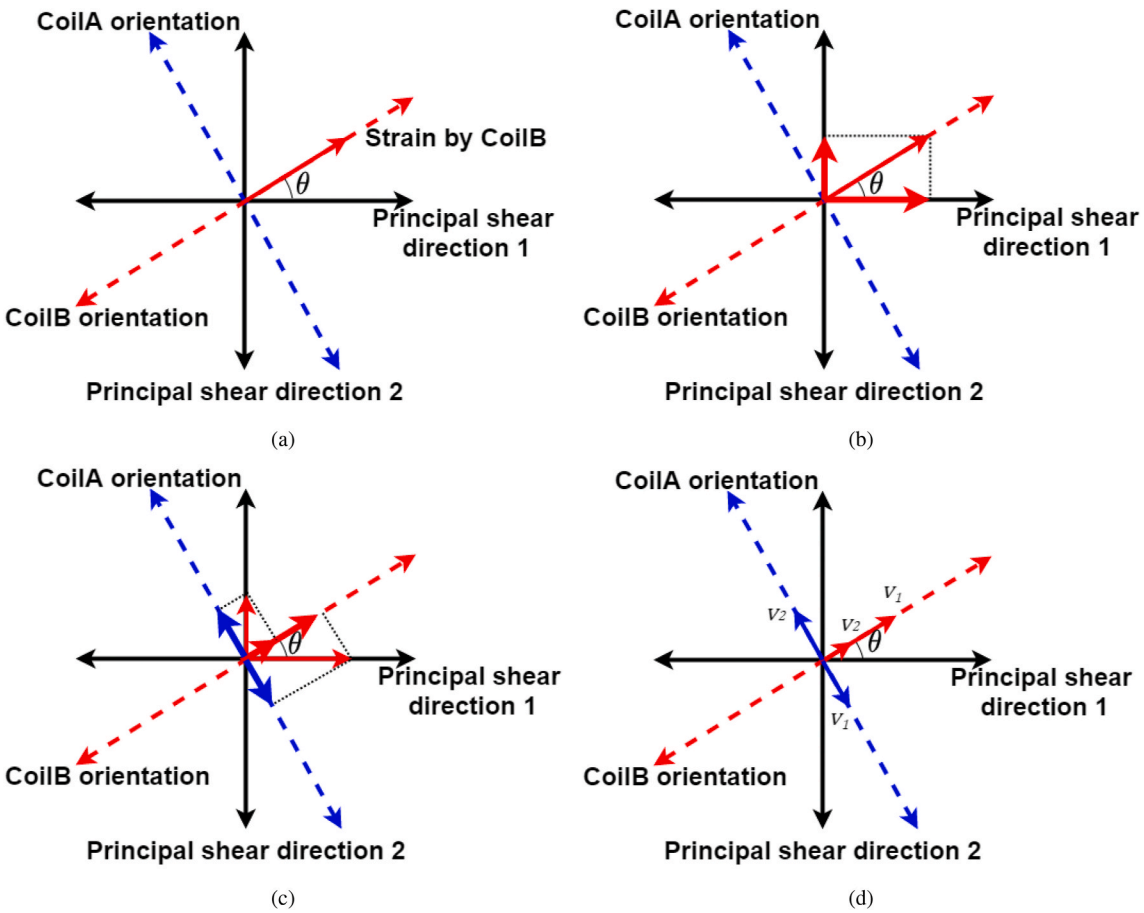


Fig. 5. Wave splitting phenomenon represented as vector quantities. a) Strain generated by the OCLC-EMAT coil B. b) The strain generated by the OCLC-EMAT coil B splitting into the two principal shear directions. c) The strain travelling on the principal shear directions projected onto the OCLC-EMAT coils. d) The shear waves measured by the OCLC-EMAT coils. The bold arrows indicate the resulting shear strain vector at each step. v_1 and v_2 indicate the wave speed of the vector component. The sub-indices 1 and 2 correspond to the wave speed of the different principal directions.

used to reconstruct a pure shear wave polarised along the PSDs without needing to physically rotating the transducer. We call this electrical steering (of the polarisation).

Two linearly polarised shear loads and co-located can be used to generate a pure shear wave polarised along only one of the principal directions in an anisotropic material. The two orthogonal shear loads can be at any angle with respect to the PSDs. However, they must be excited simultaneously and of the right relative amplitude to obtain a shear wave that propagates with a pure strain component along on of the PSDs. Once the two orthogonal and amplitude modulated shear loads are excited on top of the material, their strain components split across the two PSDs instantly. This generates two new strain components aligned with the principal directions. However, due the opposite sign of the split components along one principal direction, one of the resultant strain components is cancelled. Fig. 6 illustrates the concept.

Fig. 6a shows the strain components of the two orthogonal shear loads excited at the surface of the anisotropic material. Their amplitudes are proportional to the generated shear waves. The two shear wave strain components are oriented at an arbitrary angle θ. Fig. 6b shows the strain components of the orthogonal shear loads splitting onto the PSDs of the material. Fig. 6c displays the final result of the interaction of the strain components. The resultant strain is aligned solely with one of the two PSDs. The relationship of the resultant wave with respect to the excitation signals can be written as simple vector summations:

$$\begin{aligned} S_{comb\rightarrow PSD1} &= \overline{CoilB} * cos(\theta) - \overline{CoilA} * sin(\theta) \\ S_{comb\rightarrow PSD2} &= \overline{CoilB} * sin(\theta) + \overline{CoilA} * cos(\theta) \end{aligned} \quad (8)$$

Where $S_{comb\rightarrow PSD1}$ and $S_{comb\rightarrow PSD2}$ are the pure shear waves travelling along one of the PSDs. The sub-indices $comb\rightarrow PSD1$ and $comb\rightarrow PSD2$ identify on which PSD each wave is polarised. $\overline{CoilB}$ and $\overline{CoilA}$ represents the signals applied on the coils for the excitation. The $cos(\theta)$, $sin(\theta)$ and the $+$ and $-$ signs are the amplitude modulation needed to obtain a shear wave purely polarised along one of the PSDs.

The combination of the shear waves $S_{comb\rightarrow PSD1}$ and $S_{comb\rightarrow PSD2}$ can replicate physical excitation along any arbitrary direction on the surface of the material, hence electrical steering.

3.4. Crack detection using two orthogonal and co-located transducers

The presence of a defect can be detected using a two-step procedure: first, the shear waves strain components are aligned with the PSDs of the material. The reason for this is to isolate the interaction of the two shear waves with a defect from the effects induced by the source/receiver misalignment with the PSDs of the material. Then, in the second step, the recorded back-wall echoes are analysed and the presence of a defect in the anisotropic material is identified.

In the first step, two co-located transducers that act as shear load sources and as back-wall echo recorders are aligned with the PSDs of the material. The alignment of the transducers can be achieved by estimating the angular position of the transducers with respect to the PSDs of the anisotropic material, see section 3.2, and then rotating the transducers by the calculated angle so they are in the direction of the principal directions. By doing this, the changes on the back-wall echoes resulting from the sources/receivers misaligned with the PSDs is

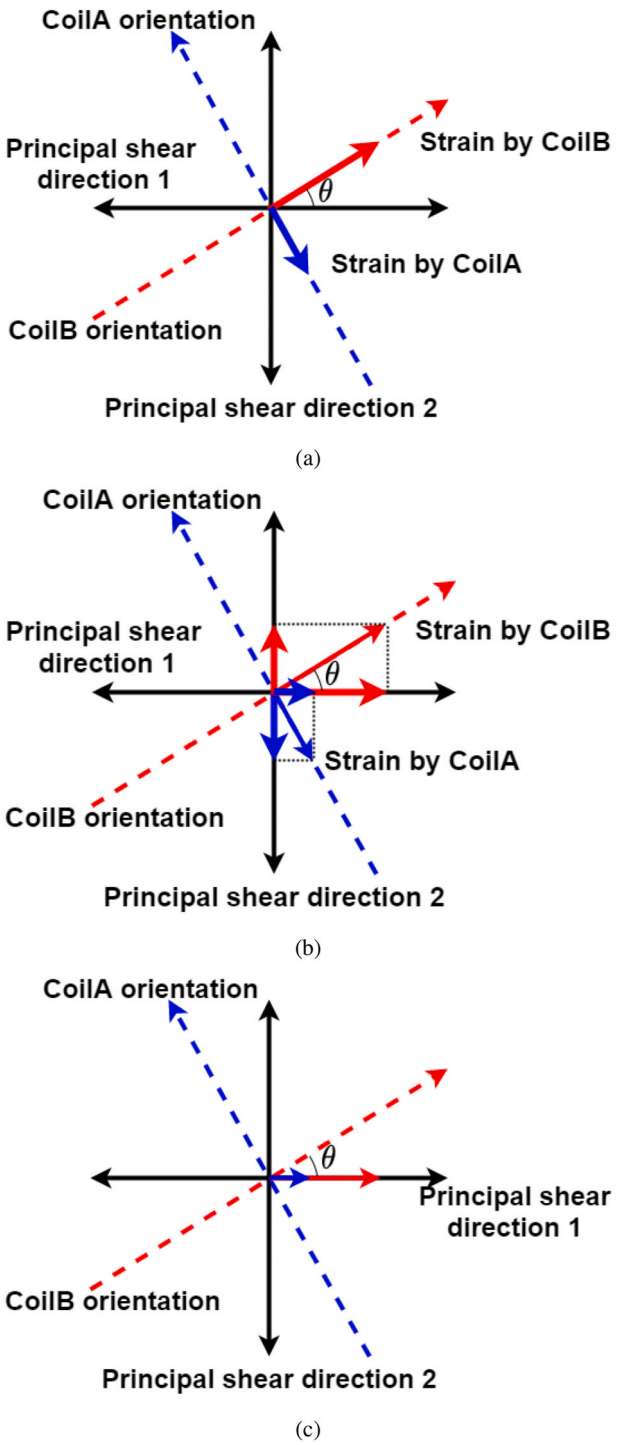


Fig. 6. Combining excitation on coil A and B to result in a pure strain aligned with the principal shear direction 1. The bold arrows indicate the resulting shear strain vector at each step. a) Strain generated by the OCLC-EMAT coils. b) The strain generated by the OCLC-EMAT coils splitting into the two principal shear directions. c) The resulting strain excited with both coils aligned with one of the principal shear directions.

minimised.

The second step consists of using the co-located transducers, already aligned in the first step, to perform a pulse-echo test in the anisotropic material. The pulse-echo test is performed by using one of the transducers as the source and the two transducers as receivers. The active transducer generates a time varying shear load along one of the principal directions. Due to the shear load polarisation's alignment with one of the PSDs, the particle displacement of the excited shear wave occurs along the same principal direction. Therefore, no shear wave with displacement polarised along the other PSD is generated. This implies that the back-wall echoes of the generated shear wave are received only by the shear load generating transducer. However, if a crack-like defect is present, the particle displacement of the generated shear wave splits into two particle displacements along the principal shear directions, once it gets in contact with the defect. The two new particle displacements generate two shear waves with polarisation direction along each PSDs. The two new shear waves bounce back to the transducers from the back-wall of the material. Therefore, when a crack-like defect is present, the back-wall echoes of the generated shear wave can be measured with the two orthogonal co-located transducers, as is shown in Fig. 7. This contracts with when the crack-like defect is not present, where the back-wall echoes of the excited shear wave is measured only by the same transducer used to generate the wave.

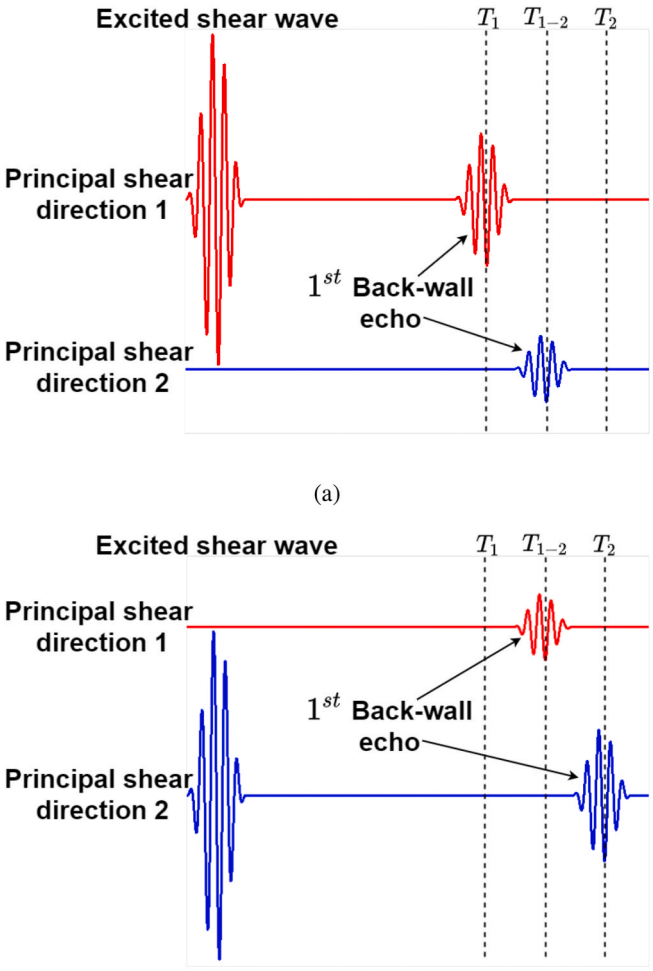


Fig. 7. Shear wave splitting into two shear waves after interaction with a crack in an anisotropic medium. The new shear wave will travel aligned with the principal shear direction. a) Shear wave excited along principal shear direction 1 and back-wall reflections measured along the two principal directions. b) Shear wave excited along principal shear direction 2 and back-wall reflections measured along the two principal directions. T_1 and T_2 indicate the arrival time at where a back-wall echo will arrive if it is travelling along the principal shear direction 1 or 2, respectively. T_{1-2} refers at the arrival time of the back-wall echo received at the principal shear direction 2 after a wave travelling along the principal shear direction 1 splits due to the presence of the crack.

3.5. Estimating the crack orientation using orthogonal and co-located shear transducers

To estimate the orientation of a crack-like defect in an anisotropic material an analysis based on the signal amplitude of the first back-wall echo of two orthogonal shear waves is proposed. The authors are proposing to study the problem using the vector representation of the superposition of two consecutive wave interactions: 1) the shear wave interacting with a tilted crack in an isotropic material and, 2) the shear wave splitting into two shear waves polarised along the PSDs. Decomposing this phenomenon into two consecutive shear wave interactions is possible when using an incident shear wave with polarisation along one of the PSDs only, and therefore the shear wave does not split due to the material, but only splits due to the presence of the crack.

The effect of the first part of the superposition study on the shear wave propagating can be explained as follows: in an isotropic medium, the amplitude signal of the first back-wall reflection, which is received after a shear wave interacted with a back-wall crack, depends on the angle formed between the shear wave source and the orientation of the crack in the material [16,23]. This relationship can be represented as the amplitude of the first back-wall echo measured with the receiver parallel and perpendicular to the crack [16] and it is shown in Fig. 8.

The consecutive second part of the superposition analysis can be explained as continues: the amplitude of the first back-wall echo, after mode conversion, of the incident shear wave is estimated as the projection of the amplitude of the back-wall reflection parallel and perpendicular to the crack onto the principal shear directions of the anisotropic material as is shown in Fig. 9. Fig. 9 illustrates the vector representation of the superposition analysis of the shear wave interacting with a crack in an anisotropic media. For illustration purposes, the OCLC-EMAT is used as the shear load source and wave receiver. The shear load is applied by coil B of the OCLC-EMAT and the first back-wall echo is received with both coils. Fig. 9a shows the strain component of the excited shear wave polarised along the PSD 1. Additionally, it represents the strain component of the excited shear wave propagating in the material while it is unperturbed by the defect. Fig. 9b displays the strain component of the excited shear wave once it gets in contact with the crack. These strain components are estimated as the back-wall reflections measured normal to and along the tilted crack in an isotropic material. Fig. 9c illustrates how the strain components generated after the incident shear wave interacts with the crack splits into two shear waves polarised along the two PSDs of the material. In Fig. 9d, the strain components of the first back-wall echo measured by the coils of the OCLC-EMAT are shown.

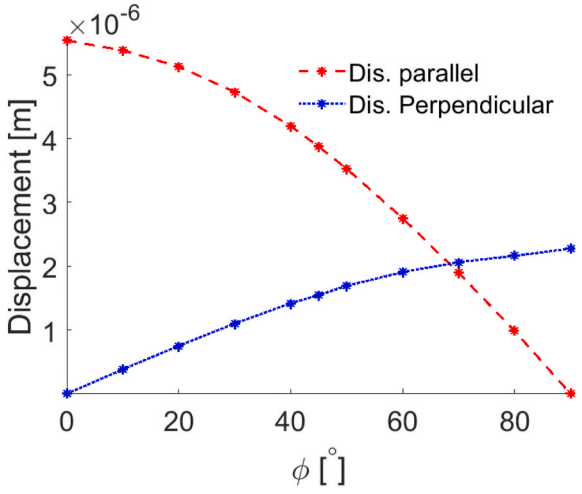


Fig. 8. Maximum amplitude of the 1st back-wall reflection measured parallel and perpendicular to the crack versus the angle of the polarisation of the incident shear wave. The results were obtained in the simulation described in Ref. [16], where the material is isotropic.

The signals recorded with the two coils, during the pulse-echo test illustrated in Fig. 9, can be expressed as the transmission of a shear wave from coil B and measured with coil B and coil A. The expression of the two transmissions can be written as:

$$CoilB \rightarrow CoilB = A_1{*}cos^2(\varphi) + A_2{*}sin^2(\varphi) \tag{9}$$

$$CoilB \rightarrow CoilA = A_1{*}cos(\varphi){*}sin(\varphi) + A_2{*}sin(\varphi){*}cos(\varphi) \tag{10}$$

Where *CoilB→CoilB* and *CoilB→CoilA* symbolise the shear wave transmission from coil B and its reception with coil B and coil A, respectively. φ is the angle formed between the crack surface and the excitation source. A_1 and A_2 Are the signal amplitude of the back-wall echoes obtained when the incident shear wave is oriented parallel and perpendicular to the crack in an isotropic material (or align with one of the principal shear directions in an anisotropic material). A_1 is the maximum amplitude of the back-wall echoes when excited along the crack with unit input and A_2 is the maximum amplitude of the back-wall echoes when excited perpendicular to the defect with a unit input.

Similar to the pulse-echo test illustrated in Fig. 9, the second pulse-echo test can be indicated as the transmission of a shear wave from coil A to coil B and coil A. The transmission/reception of the shear wave can be written as:

$$CoilA \rightarrow CoilB = A_1{*}cos(\varphi){*}sin(\varphi) + A_2{*}cos(\varphi){*}sin(\varphi) \tag{11}$$

$$CoilA \rightarrow CoilA = A_1{*}sin^2(\varphi) + A_2{*}cos^2(\varphi) \tag{12}$$

Where *CoilA→CoilB* and *CoilA→CoilA* represent the signal measured when a shear wave is transmitted from coil A and received with coil B and coil A, respectively.

The orientation of the crack-like defect, illustrated in Fig. 9, can be estimated from equations (9) and (12) as follows:

$$\varphi = tan^{-1}\sqrt{\frac{1 - A_2 \Big/ A_1 {*}\frac{CoilA\rightarrow CoilA}{CoilB\rightarrow CoilB}}{\frac{CoilA\rightarrow CoilA}{CoilB\rightarrow CoilB} - A_2 \Big/ A_1}} \tag{13}$$

The steps followed in order to obtain equation (13) are shown in appendix A. Equation (13) assumes that the amplitude of the strain components applied at the principal directions are equal. In case, that strain components are not equal, the amplitude signal of the back-wall echoes, *CoilA→CoilA*, needs to be normalised with respect to *coilB*. The normalisation can be carried out by multiplying *CoilA→CoilA* with $\frac{CoilB\rightarrow CoilA}{CoilA\rightarrow CoilB}$.

Additionally, prior information of the values A_1 and A_2 are required in order to calculate the crack orientation. For the work presented in this paper, A_1 and A_2 were obtained from the experimental results shown in paper [16].

4. Experimental results

The results presented in this section were obtained from experiments that mimic the theory presented in section 3.

The experimental setup used to perform the experiments was similar to the one described in paper [16]; but with the difference that the orientation of the notches machined, in the aluminium blocks, were changed. The orientation (φ) of the inspected notches were 0°, 20°, 30°, 45°, 60°, 70° and 90°. In total, 4 different samples were inspected. On each one a single notch was machined. The notches were machined on the back-wall of the blocks. The notch dimensions were 5*mm* by 0.3 mm (depth, width) and they ran across the whole specimen (aluminium block) as indicated in Fig. 10. The results obtained with notches oriented at 60°, 70° and 90° were achieved on the same blocks as for notches

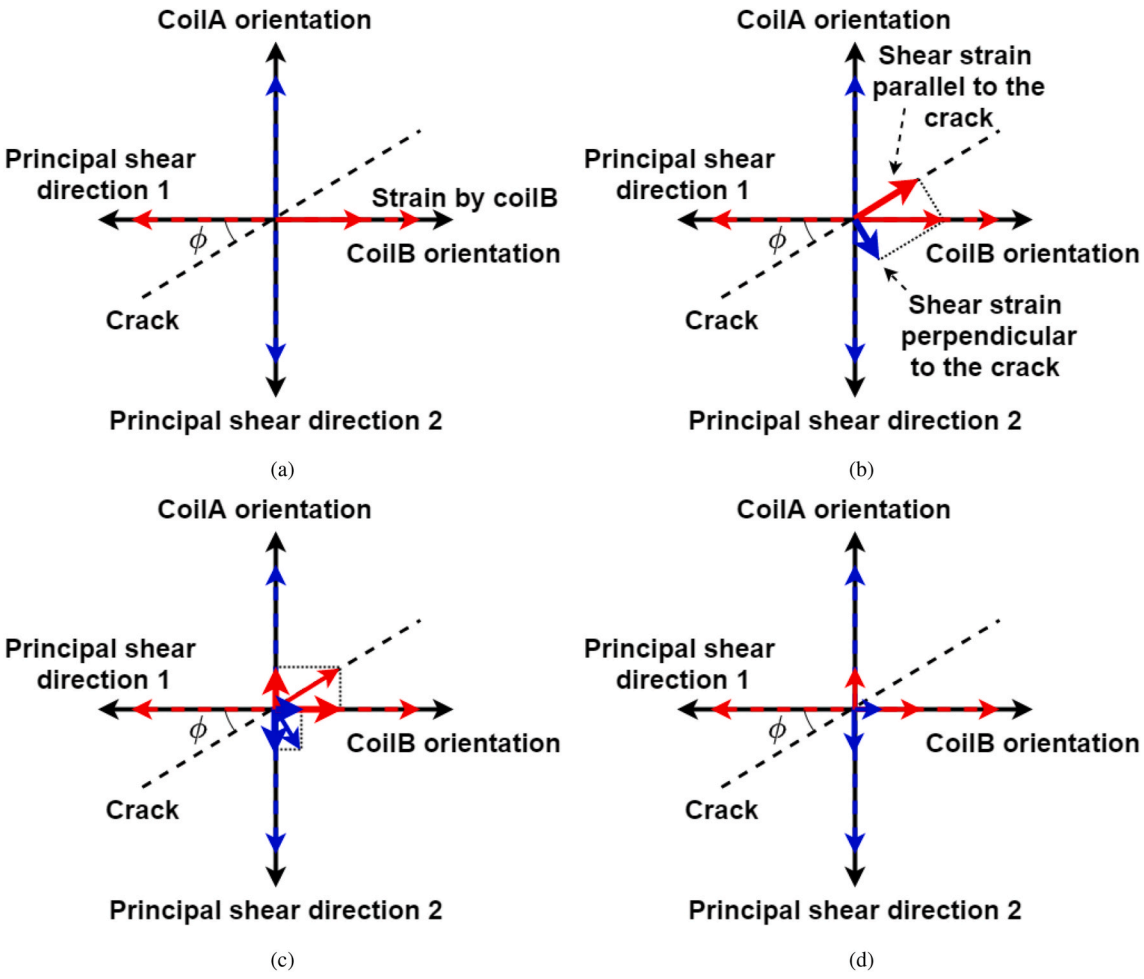


Fig. 9. Vector representation of the shear wave interacting with the crack as the superposition of two wave interactions: the amplitude of the back-wall reflection in an isotropic material and the shear wave splitting in an anisotropic material. The bold arrows indicate the resulting shear strain vector at each step. a) Strain generated by coil B of the OCLC-EMAT. b) Strain components generated at the crack after the shear wave propagating along the principal shear direction 1 interacts with the defect. c) Projection of the shear strain components generated at the crack onto the principal shear directions of the anisotropic material. d) The strain measured by the coils of the OCLC-EMAT.

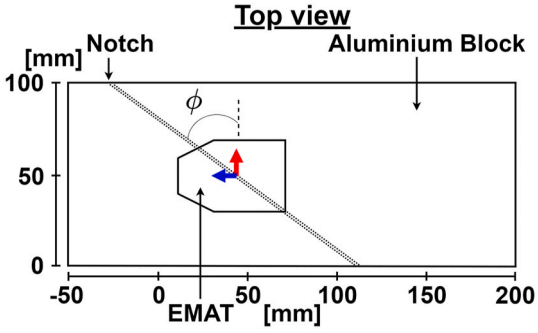


Fig. 10. Schematic Top view of the test carried out to characterise the notch orientation.

oriented at 30°, 20° and 0°, respectively; but with the OCLC-EMAT rotated 90° with respect to the position used on the experiments for 30°, 20° and 0°. Fig. 10 is a schematic top view of the experiments carried out to estimate the notch orientation in an anisotropic material.

As is shown in Fig. 10, the notches were machined on the left side of the aluminium block, leaving the right side of the block as the test zone used to characterise the orientation of the principal shear directions of the material.

Fig. 11 shows the estimated orientation of the PSDs of the material as the OCLC-EMAT is rotating on top of the aluminium block. θ is the existing angle formed by the OCLC-EMAT coils with the principal

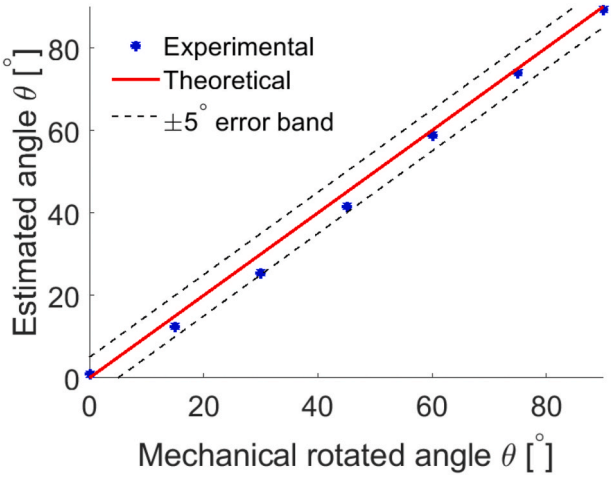


Fig. 11. Estimated orientation of principal shear directions of an anisotropic material (aluminium) with respect to the OCLC-EMAT coils.

directions. The red line indicates the angle form by the physical position of the OCLC-EMAT coils and the PSDs, the blue dots are the estimated angle formed by the OCLC-EMAT coils with the principal shear directions and the black dashed line are the 5° upper and lower error band. Fourteen pulse-echo tests were performed in total.

Fig. 12 displays the results obtained when two orthogonal shear loads were used to excite a single shear wave polarised along one of the principal shear directions. The pulse-echo tests were carried out on an area where the notches were not present. Fig. 12a shows a comparison of two different pulse-echo tests, when the OCLC-EMAT was physically at θ equal to 0° and 30°. To excite one shear wave polarised along the first principal direction, when θ is 30°, the signal amplitude of the shear loads were modulated according to equation (8). The back-wall echoes of the excited shear wave are recorded using the two coils of the OCLC-EMAT. The time-traces plotted in Fig. 12a are the sum of the signal measured with both coils during a single pulse-echo test. Fig. 12b shows the calculated ToF of the back-wall echoes obtained when the shear wave is excited along the principal shear directions. The shear wave was excited using two orthogonal shear loads. The tractions were excited at different angles with respect to the PSDs. The different angles were obtained by rotating the OCLC-EMAT on top of the aluminium block. The black line indicates the wave speed measured when the shear surface tractions were polarised along the principal shear directions 1 and 2. The blue circles are the measured wave velocity of the shear wave polarised along the PSD 1 at different θ. The red dots are the calculated wave speed of the shear wave polarised along PSD 2 for different θ angles and the dashed black line are the 0.5% upper and lower error band of the wave speed. Sixteen pulse-echo tests were performed in total.

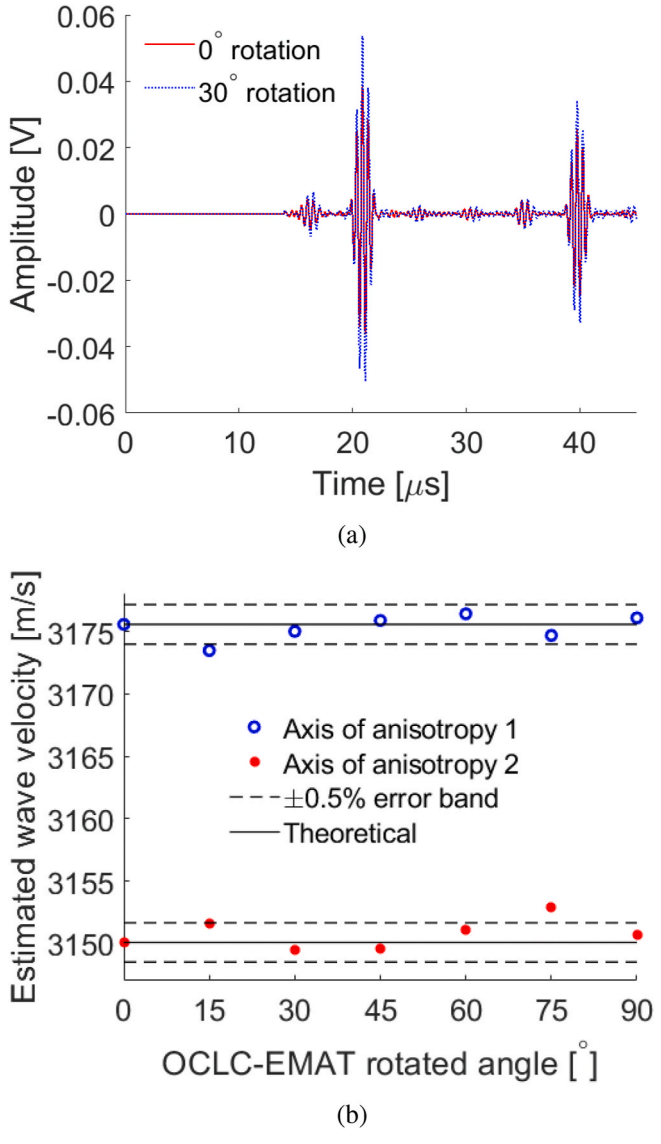


Fig. 12. Experimental results of shear waves oriented along the principal shear directions. The shear waves were excited using two orthogonal shear loads. The results were obtained with different OCLC-EMAT angular positions. a) A-scans of excited shear wave travelling aligned with the principal shear direction 1. b) Wave speed estimation of the excited shear waves travelling along the principal shear directions of the anisotropic material.

In Fig. 13, the time-traces obtained after one pulse-echo test are shown to indicate the presence of a notch. The signals displayed are the result of a shear wave interacting with a notch present in an anisotropic material. The defect was oriented 20° with respect to the principal shear direction 1 of the material. The pulse-echo test was carried out with the OCLC-EMAT coils aligned with the PSDs. The shear wave was excited with coil B of the OCLC-EMAT and its back-wall echoes were recorded with both coils. As mentioned in section 3.4, when the defect is not present in the area where the pulse-echo test is carried out, the received back-wall echoes are only measured with one coil, as shown in Fig. 4a while, when the defect is present, the back-wall echoes received after the interaction of the shear wave with the notch are recorded with both coils of the OCLC-EMAT, as is shown in Fig. 13. One pulse-echo test was performed to obtain the results shown in Fig. 13.

Fig. 14 displays the results obtained after the inspection of an anisotropic material with notches machined at different angles. The results were obtained by using an OCLC-EMAT on top of the area where the notch was present. The transducer's coils were placed with orientation along the principal shear directions of the material. The inspection of each crack-like defect was carried out by mimicking the steps described in section 3.5. Fig. 10 shows the schematic top view of the inspection. The OCLC-EMAT is placed on top of the aluminium block and aligned with the PSDs on an area where the defect is present. Fig. 14 summarises the estimated notch angles. The results were obtained by performing pulse-echo tests in the inspected material. The red line in the plot indicates the orientation on which the notches were machined with respect to first principal shear direction, while the blue dots are the estimated notch orientation and the dashed black line are the 5° upper and lower error band of the estimation. Fourteen pulse-echo tests were performed in total, two for each estimated notch orientation.

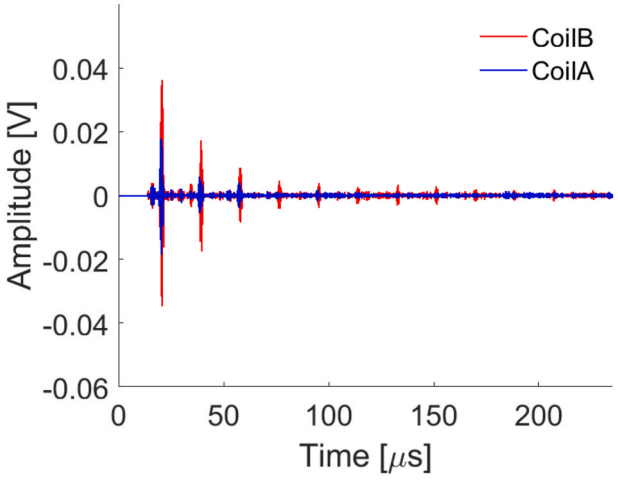


Fig. 13. Experimental results of notch detection based on back-wall reflection. The notch was oriented 20° away from the first principal direction of the material. The results obtained, in contrast to the signals shown in Fig. 4a, display an amplitude and shape change among the recorded signals. The back-wall echoes are received with both coils of the OCLC-EMAT.

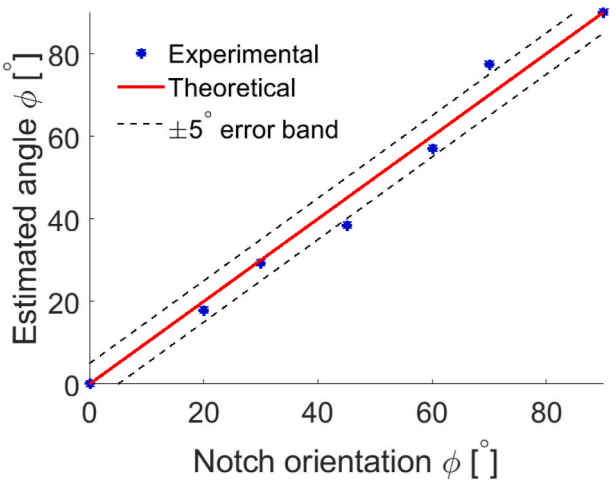


Fig. 14. Experimental characterisation of the notch orientation. The notch estimated orientation was measured with respect to the first principal shear direction.

5. Discussion

The work presented in this paper establishes a simple method of characterising the level of anisotropy and the principal shear directions of a material. The characterisation of the level of anisotropy and the orientation of the principal shear directions are achieved by measuring a shear wave splitting in the material. These serve the purpose of crack-like defect detection in this paper, but they may have a broader applications in the field of material characterisation (e.g. to inspect the homogeneity of larger samples, monitor the level of strains in a material, measuring residual stresses, etc).

In the presented work, the crack-like defect detection and the evaluation of its orientation in anisotropic media relies on the prior knowledge of the principal shear directions, which is obtained by characterising the material on a neighbouring region without defects. However, real applications may encounter situations more complicated than what we have assumed here. For instance, the access to defect-free areas might be restricted, or whether an area has a defect or not could be unknown beforehand. In addition, the orientation of the PSDs may vary from one area to another due to factors such as grain micro-structural variations, localised inclusions in the material, or residual or thermally induced stresses, etc. We will aim to address these difficulties in future work by building up on the findings presented here. For example, we will explore the combination of two pairs of OCLC coils aligned with 45° equal gaps and study the differences between the signals from the pairs. We believe a system like this could be able to 1) characterise the PSDs of the shear waves, 2) determine whether a crack-like defect is present, 3) obtain the orientation of the crack if indeed present, all at the same time, which is an exciting and useful prospect to pursue.

The compensation of the received signals proposed in section 3.5, used to estimate the orientation of the defect, assumes that the amplitude difference in the back-wall echoes is the result of the coils not being at the same lift-off with respect to the material. The compensation also assumes that the signals in equations (2) and (3) are equal. However, if the signals expressed in equations (2) and (3) are not equal due to the material anisotropy, the compensation method presented can be used to compensated this variation. In this case, the amplitude difference of the shear surface tractions needs to be eliminated before starting the inspection. In addition, in our theories and experiments, we have used bare metals without painting, so the reflection coefficients remain uniform; for real-world applications involving surface painting or other surface treatments that may affect the reflection amplitudes, more comprehensive investigations will be needed.

6. Conclusion

A methodology to detect and characterise the orientation of crack-like defects in anisotropic materials was presented. The proposed method utilises two orthogonal and co-located shear waves with linear polarisation to inspect the anisotropic material. With the use of two shear waves it was possible to establish the level of anisotropy of a material, the orientation of the principal shear directions of the material, to detect the presence of a crack-like defect and to estimate the defect orientation with respect to the principal directions. The results obtained show the efficacy of the proposed method on an aluminium block. The orientation of the principal shear directions could experimentally be determined within $\sim \pm 5^{\circ}$ error and the level of anisotropy of the material to $\sim 0.5\%$. Moreover, the notches orientation could be estimated experimentally within $\sim \pm 5^{\circ}$.

To understand the interaction of the two orthogonal shear waves in the anisotropic material and with a crack-like defect, a study of the two waves propagating in the material was presented. The study was based on vector analysis of the strain components of the two shear waves travelling through the anisotropic material. The representation of the strain components of the shear waves as vector quantities allowed the estimation of the anisotropic material characteristics, as well as the estimation of the orientation of crack-like defects.

Finally, the results obtained in this work showed agreement with the theory proposed. The detection methodology of crack-like defects with two orthogonal and co-located shear waves was extended to anisotropic materials. Additionally, the concept of estimating the defect orientation with respect to the principal axes of the material was added to the methodology.

CRediT authorship contribution statement

Jaime Parra-Raad: Conceptualization, Investigation, Formal analysis, Validation, Writing – original draft. **Bo Lan:** Conceptualization, Investigation, Formal analysis, Validation, Writing – original draft. **Frederic Cegla:** Conceptualization, Investigation, Formal analysis, Validation, Writing – original draft.

Declaration of competing interest

The authors declare that they have no known competing financial interests or personal relationships that could have appeared to influence the work reported in this paper.

Acknowledgements

The authors would like to acknowledge funding from the ORCA hub (EPSRC grant EP/R026173/1) and Permasense Ltd.

Appendix A. Calculating the orientation angle of a crack-like defect

The orientation angle of a crack-like defect was defined as the angle form between the crack-like defect and one of principal shear directions of the anisotropic material. It is illustrated as φ in Fig. 9 and in Fig. 10. The mathematical formula used in this paper to estimate the orientation angle is equation (13). In this appendix, it is summarised the mathematical steps used to obtain the equation mentioned before. Equation (13) was obtained by

following the next steps:

$$\frac{CoilA\rightarrow CoilA}{CoilB\rightarrow CoilB}=\frac{\left[A_1{*}cos^2(\varphi)+A_2{*}sin^2(\varphi)\right]}{\left[A_1{*}sin^2(\varphi)+A_2{*}cos^2(\varphi)\right]}$$

$$\frac{CoilA\rightarrow CoilA}{CoilB\rightarrow CoilB}=\frac{\left[cos^2(\varphi)+A_2/A_1{*}sin^2(\varphi)\right]}{sin^2(\varphi)+A_2/A_1{*}cos^2(\varphi)\right]}$$

$$\frac{CoilA\rightarrow CoilA}{CoilB\rightarrow CoilB}=\frac{\left[1+A_2/A_1{*}tan^2(\varphi)\right]}{\left[tan^2(\varphi)+A_2/A_1\right]}$$

$$\left[tan^2(\varphi)+A_2/A_1\right]{*}\frac{CoilA\rightarrow CoilA}{CoilB\rightarrow CoilB}=$$

$$1+A_2/A_1{*}tan^2(\varphi)$$

$$tan^2(\varphi)=\frac{1-A_2\Big/A_1{*}\dfrac{CoilA\rightarrow CoilA}{CoilB\rightarrow CoilB}}{\dfrac{CoilA\rightarrow CoilA}{CoilB\rightarrow CoilB}-A_2\Big/A_1}$$

$$\varphi=tan^{-1}\sqrt{\frac{1-A_2\Big/A_1{*}\dfrac{CoilA\rightarrow CoilA}{CoilB\rightarrow CoilB}}{\dfrac{CoilA\rightarrow CoilA}{CoilB\rightarrow CoilB}-A_2\Big/A_1}}$$

References

[1] Voigt Thomas, Ye Guang, Sun Zhihui, Surendra P. Shah, and Klaas [van Breugel]. Early age microstructure of portland cement mortar investigated by ultrasonic shear waves and numerical simulation. Cement Concr Res 2005;35(5):858–66.

[2] Ruiz Alberto, Ortiz Noemi, Carreón Hector, Rubio Carlos. Utilization of ultrasonic measurements for determining the variations in microstructure of thermally degraded 2205 duplex stainless steel. J Nondestr Eval 2009;28(131).

[3] Zhang Jie, Song Yongfeng, Li Xiongbing, Zhong ChengHuan. Comparison of experimental measurements of material grain size using ultrasound. J Nondestr Eval 2020;39.

[4] Maki Carson T, Michaels Jennifer E, Weng Yu, Michaels Thomas E. Angle-beam shear wave scattering from buried crack-like defects in bonded specimens. AIP Conf Proc 2017;1806(1):020003.

[5] Ogilvy JA, Temple JAG. Diffraction of elastic waves by cracks: application to time-of-flight inspection. Ultrasonics 1983;21(6):259–69.

[6] Baskaran G, Krishnan Balasubramaniam, [Lakshmana Rao] C. Shear-wave time of flight diffraction (s-tofd) technique. NDT E Int 2006;39(6):458–67.

[7] Chua CA, Cawley P. Crack growth monitoring using fundamental shear horizontal guided waves. Struct Health Monit 2019;2020:1311–22.

[8] Xiang L, Edwards RS. Multiple wavemode scanning for near and far-side defect characterisation. J Nondestr Eval 2020;39.

[9] Allen DR, Sayers CM. The measurement of residual stress in textured steel using an ultrasonic velocity combinations technique. Ultrasonics 1984;22(4):179–88.

[10] King RB, Fortunko CM. Determination of in-plane residual stress states in plates using horizontally polarized shear waves. J Appl Phys 1983;54(6):3027–35.

[11] Crecraft DI. The measurement of applied and residual stresses in metals using ultrasonic waves. J Sound Vib 1967;5(1):173–92.

[12] Love Augustus. A treatise on the mathematical theory of elasticity. 1892. hal-01307751f.

[13] Silver Paul G, Savage Martha K. The interpretation of shear-wave splitting parameters in the presence of two anisotropic layers. Geophys J Int 1994;119(3):949–63. 12.

[14] Datta SK, Shah AH, Fortunko CM. Diffraction of medium and long wavelength horizontally polarized shear waves by edge cracks. J Appl Phys 1982;53(4):2895–903.

[15] Standard guide for planar flaw height sizing by ultrasonics. West Conshohocken, PA, USA: Standard, ASTM International; mar 2018.

[16] Parra-Raad Jaime, Khalili Pouyan, Cegla Frederic. Shear waves with orthogonal polarisations for thickness measurement and crack detection using emats. NDT E Int 2020;111:102212.

[17] Haslinger Stewart G, Lowe Michael JS, Huthwaite Peter, Craster Richard V, Fan Shi. Elastic shear wave scattering by randomly rough surfaces. J Mech Phys Solid 2020;137:103852.

[18] Guo Wei, Gao Bin, Tian Gui Yun, Si Dan. Physic perspective fusion of electromagnetic acou stic transducer and pulsed eddy current testing in non-destructive testing system. Phil Trans Math Phys Eng Sci 2020;378(2182):20190608.

[19] Fourmeau M, Børvik T, Benallal A, Lademo OG, Hopperstad OS. On the plastic anisotropy of an aluminium alloy and its influence on constrained multiaxial flow. Int J Plast 2011;27(12):2005–25 [Special Issue In Honor of Nobutada Ohno].

[20] Isla J, Cegla F. Optimization of the bias magnetic field of shear wave emats. IEEE Trans Ultrason Ferroelectrics Freq Contr Aug 2016;63(8):1148–60.

[21] Sondergeld CH, Rai CS. Laboratory observations of shear-wave propagation in anisotropic media. Lead Edge 1992;11(2):38–43.

[22] Johnson George C, Mase G Thomas. Acoustoelasticity in transversely isotropic materials. J Acoust Soc Am 1984;75(6):1741–7.

[23] Harker AH. Numerical modelling of the scattering of elastic waves in plates. J Nondestr Eval Jun 1984;4(2):89–106.